Correlation of the Phosphorylation States of pp60^{c-src} with Tyrosine Kinase Activity: The Intramolecular pY530−SH2 Complex Retains Significant Activity If Y419 Is Phosphorylated†

Renee J. Boerner, Daniel B. Kassel,‡ Sean C. Barker, Byron Ellis, Pam DeLacy,§ and Wilson B. Knight*

Departments of Biochemistry and Bioanalytical Chemistry, Glaxo Wellcome Inc., Research Triangle Park, North Carolina 27709

Received February 1, 1996; Revised Manuscript Received April 17, 1996⊗

ABSTRACT: Rapid digestion of pp60^{c-src} tyrosine kinase (*src* TK) in combination with electrospray ionization mass spectrometry enabled the determination of the time course for autophosphorylation of three tyrosine sites (Y338, Y419, and Y530) and a correlation with *src* TK activity. A form of *src* TK was purified from baculovirus-infected cells which contains only Y338 partially phosphorylated. Incubation with MgATP increases the phosphorylation of all three sites. The autophosphorylation and dephosphorylation of Y419 are directly correlated with the level of *src* TK activity. The role of Y338 phosphorylation is unknown. Conditions resulting in complete autophosphorylation of Y530 were identified by electrospray ionization mass spectrometry. Surface plasmon resonance detection and size exclusion chromatography provide direct evidence for an intramolecular pY530−SH2 complex, supporting previous models [Matsuda, M., Mayer, B. J., Fukui, Y., & Hanafusa, H. (1990) *Science 248*, 1537−1539]. Contrary to these models, when the enzyme is fully phosphorylated on Y530, phosphorylated on Y419, and present only as the intramolecular pY530−SH2 complex, 20% of the kinase activity is retained. In addition, the K_m's for substrates are unaffected. Disruption of the pY530−SH2 interaction and activation of kinase activity by a high-affinity SH2 ligand yield a $K_{activation}$ which is 200-fold larger than the K_d for ligand binding to the uncomplexed *src* SH2 domain. These data suggest a K_{eq} of 200 (unitless) for the intramolecular association of pY530 with the SH2 domain. We propose that the pY530−SH2 interaction modulates signal transduction by down-regulating *src* TK activity 5-fold, and perhaps more importantly by inhibiting protein−protein interactions with the SH2 domain. These results have significant implications relative to the development of SH2 ligands as therapeutics to control aberrant signal transduction. These ligands will be 200-fold less effective at inhibiting protein−protein interactions versus down-regulated *src* TK than versus activated *src* TK. This should minimize activation of *src* TK activity in normal cells and lead to an increased therapeutic index.

The phosphorylation and dephosphorylation of proteins play a major role in signal transduction pathways. The protein kinases responsible for these phosphorylation events are often themselves controlled by phosphorylation. In fact, many of the protein tyrosine kinases undergo autophosphorylation. One proposed function for these tyrosine autophosphorylations is to provide docking sites for SH2[1] -containing proteins (Cantley et al., 1991). Many of the protein tyrosine kinases, including pp60^{c-src} tyrosine kinase (*src* TK), contain both tyrosine autophosphorylation sites and SH2 domains, as well as SH3 domains [for a review of nonreceptor tyrosine kinases, see Bolen (1993) and Sudol (1993)]. *Src* TK undergoes autophosphorylation on Y419, located within the tyrosine kinase domain, which leads to activation of enzymatic activity. *Src* TK contains a second tyrosine phosphorylation site, Y530, which was shown to negatively regulate *src* TK activity [for a review, see Cantley et al. (1991) and Cooper and Howell (1993)]. Intramolecular binding of phosphorylated Y530 to the *src* SH2 domain resulting in blocking of the catalytic site was proposed as the mechanism for down-regulation (Matsuda et al., 1990). Although it was proposed that *in vivo* phosphorylation of Y530 is catalyzed by an exogenous kinase (Okada & Nakagawa, 1989; Nada et al., 1991), *in vitro* and *in vivo* autophosphorylation of Y530 has also been demonstrated (Cooper & King, 1986; Cooper & MacAuley, 1988). A third tyrosine phosphorylation site has previously been identified, although its functional significance is not known (Barker et al., 1995).

In this work, the time courses for autophosphorylation and dephosphorylation are examined. This enables the identification of conditions which give rise to differentially phosphorylated enzyme forms. These enzyme forms were then used to determine the functional significance of tyrosine phosphorylation.

† A preliminary abstract of this report was submitted to the American Society for Biochemistry and Molecular Biology.

* Address correspondence to this author.

‡ Current address: CombiChem, Inc., San Diego, CA 92121.

§ Current address: PeproTech Inc., Rocky Hill, NJ 08553.

⊗ Abstract published in *Advance ACS Abstracts,* July 1, 1996.

[1] Abbreviations: CSK TK, C-terminal pp60^{c-src} tyrosine kinase; ESI-MS, electrospray ionization mass spectrometry; Hepes, *N*-(2-hydroxyethyl)piperazine-*N*′-2-ethanesulfonic acid; LDH, lactate dehydrogenase; MS/MS, tandem mass spectrometry; NADH, reduced nicotinamide adenine dinucleotide; PEP, phosphoenolpyruvate; PK, pyruvate kinase; SH2, pp60^{c-src} homology domain 2; SH3, pp60^{c-src} homology domain 3; *src* TK, pp60^{c-src} tyrosine kinase; TFA, trifluoroacetic acid.

S0006-2960(96)00248-6 CCC: $12.00

MATERIALS AND METHODS

Materials. ATP, PEP, PK, LDH, and BSA were purchased from Sigma Chemical Co. or Boehringer Mannheim. $(FGE)_3Y(GEF)_2GD$, TSTEPQYQPGENL, and TSTEPQ-pY-EEIENL were purchased from Zeneca Bioproducts (Wilmington, DE). RRLIEDAEYAARG was purchased from Bachem (CA).

Protein Expression and Purification. Src TK was expressed in baculovirus expression system as the N-85 protein deletion mutant and purified according to Ellis et al. (1994). This protein lacks the first 85 residues at the amino terminus and behaves similarly to protein expressed from a full-length construct that lacks the myristylation site (Barker et al., 1995). The amino acids are numbered according to the full length wild-type human sequence.

Electrospray Ionization Mass Spectrometry. Untreated or autophosphorylated *src* TK (75 pmol) was injected directly onto a 750 μm × 10 cm Poroszyme perfusion column which contained immobilized trypsin (PerSeptive Biosystems, Cambridge, MA), equilibrated in digestion buffer (50 mM NH_4HCO_3, 1 mM $CaCl_2$, pH 8.5). The column was housed in an oven compartment at 50 °C of an HP1090 microbore HPLC, and eluted with a flow rate of 50 μL/min. This flow rate corresponded to an analyte residence time of approximately 1 min. Protein digests were collected and analyzed by reverse phase HPLC ESI-MS using a 15 cm × 250 μm Poros R2/H perfusion column. A fast linear gradient of 1−21% buffer B in 5 min and 21−46% buffer B in 15 min was used. (Buffer A was 0.05% TFA in H_2O, and buffer B was 90/10 MeCN/H_2O containing 0.035% TFA.) A PE-Sciex API III triple quadrupole mass spectrometer (Thornhill, Ontario, Canada) was used to acquire all mass spectral data. The mass spectrometer was scanned from *m/z* 400 to 1900 in 3 s using a step size of 0.5 Da and a dwell time of 1.0 ms. The ion multiplier was set to −4800 V, and the resolution was set nominally to 1000 (50% half-height). The extent of peptide phosphorylation and dephosphorylation was determined from either UV absorbance and/or integration of the individual ion chromatograms.

Spectrophotometric Tyrosine Kinase Assays. Tyrosine kinase assays were performed as in Barker et al. (1995) and Edison et al. (1995). The phosphorylation of peptides RRLIEDAEYAARG or $(FGE)_3Y(GEF)_2GD$ and concomitant production of ADP were coupled to the oxidation of NADH using PEP, PK, and LDH. The decrease in absorbance at 340 nm was followed using a Molecular Devices (Menlo Park, CA) THERMOmax plate reader. Reaction mixtures contained 100 mM Hepes, pH 7.5, 20 mM $MgCl_2$, 100 μM DTT, 20 μg of BSA/mL, 1 mM PEP, 240 μM NADH, 45−65 units of LDH/mL, 15−30 units of PK/mL, and varying concentrations of ATP and peptide. Assays were initiated with *src* TK. Initial rates were determined by a linear least-squares fit of the absorbance versus time data. The kinetic parameters were determined by nonlinear regression analysis of the rates as a function of substrate concentration (eq 1). The $K_{activation}$ was determined by nonlinear regression analysis of the rates as a function of SH2 ligand concentration (eq 2). Nonlinear regression was conducted using GraFit (Leatherbarrow, 1992).

$$v = V_{max}[S]/(K_m + [S]) \quad (1)$$

$$v_a = V_{act}[L]/(K_{act} + [L]) \quad (2)$$

In eqs 1 and 2, v is the measured velocity, v_a is the velocity measured in the presence of SH2 ligand minus the velocity measured in the absence of SH2 ligand, V_{max} is the maximum velocity, V_{act} is the maximal activated velocity minus the velocity measured in the absence of SH2 ligand, [S] is the substrate concentration; [L] is the SH2 ligand concentration, K_m is the Michaelis constant for the varied substrate, and K_{act} is the activation constant for the SH2 ligand.

Surface plasmon resonance detection [for reviews of this technique, see Malmquist (1993) and Fagerstam et al. (1992)] was used to measure the binding of *src* TK to an immobilized phosphopeptide. The phosphopeptide was immobilized on a sensor chip surface by covalent coupling to a carboxylated dextran matrix attached to the surface. The change in optical signal as binding occurs is proportional to the mass bound and can be monitored in real time. Two peptides were immobilized on separate flow cells of the same sensor chip. TSTEPQYQPGENL, which corresponds to the C-terminus of *src* TK, was used as a control nonphosphorylated peptide, and TSTEPQ-pY-EEIENL was used as the phosphorylated peptide. To immobilize the peptides, the carboxyl groups of the Biacore CM5 sensor chip hydrogel matrix were activated with a mixture of 50 mM *N*-hydroxysuccinimide and 200 mM *N*-ethyl-*N*′-(3-diethylaminopropyl)carbodiimide for 12 min. Peptides were dissolved in 10 mM Hepes, pH 8.0, 1 M NaCl at a concentration of 0.5 mg/mL, and then injected onto the sensor chip for 20 min at a flow rate of 5 μL/min. The high salt concentration was used to overcome the negative charges of the peptide and sensor chip matrix. Unreacted groups were deactivated with a 13 min injection of 1 M ethanolamine hydrochloride, pH 8.5, following the peptide injection. This surface could be regenerated after each binding cycle with 100 mM NaOH, 0.5 M NaCl. The Biacore running buffer used for immobilization and binding studies contained 10 mM Hepes, pH 7.4, 150 mM NaCl, and 0.05% v/v of a 10% P-20 surfactant solution.

Src TK was injected over the sensor chips containing phosphopeptide and control peptide simultaneously for 1 min at a flow rate of 10 μL/min. The temperature at the sensor chip surface was set at 7 °C to inhibit any dephosphorylation of the immobilized phosphopeptide by *src* TK (Boerner et al., 1995a,b). Data points were taken when the responses reached steady-state. Eight different *src* TK concentrations ranging from 0.05 to 2.0 μM were used. As a control, 0.05 μM *src* TK was both the first and last sample to be run and gave similar results for both runs, indicating that the sensor chip was not significantly changed during the course of each individual experiment. The relationship between the net steady-state response of the kinase binding to the phosphopeptide (response minus the response to the control peptide) and concentration was fit to the Hill equation (eq 3).

$$R = R_{max}C^n/(K_d^n + C^n) \quad (3)$$

In eq 3, R is the steady-state response, C is the concentration

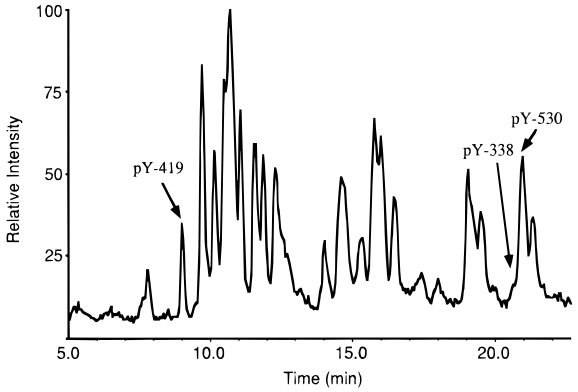

FIGURE 1: Total ion current chromatogram of a Poroszyme 2 min tryptic digest of autophosphorylated *src* TK (10 μM *src* TK, 20 mM $MgCl_2$, 1 mM ATP at 25 °C for 30 min) separated on a Poros R2/H capillary perfusion column. The phosphotyrosine-containing peptides are identified.

of *src* TK, R_{max} is the calculated maximum response, n is the Hill coefficient, and K_d is the equilibrium dissociation constant.

Analytical Size Exclusion Chromatography. One hundred microliters containing 2−5 μg of *src* TK was injected onto a Tosohaas G3000SW size exclusion column (7.5 mm i.d. × 60 cm, particle size 10 μm), and eluted with 0.3 M NaCl, 25 mM Hepes, pH 7.0, at 0.5 mL/min. Protein standards (BioRad) were used for molecular weight calibration.

Phosphorylation of Protein Substrates by Src TK. *Src* TK was autophosphorylated as mentioned in the text, except that 0.01 μCi of [γ-^{32}P]ATP/nmol of ATP was added. Autophosphorylated *src* TK (0.2 μM) was incubated with 100 μM ATP, 0.1 μCi of [γ-^{32}P]ATP/nmol of ATP, 20 mM $MgCl_2$, 1 mM vanadate, 100 mM Hepes, pH 7.5, and 0.4 mg/mL casein in a total volume of 50 μL. Reactions were incubated at 25 °C and stopped at 5 min by the addition of 2× SDS−PAGE sample buffer containing β-mercaptoethanol (Laemmli, 1970). After boiling for 5 min, samples were fractionated by 12% SDS−PAGE (BioRad). Gels were dried using a drying solution (Novex, San Diego, CA) and exposed to film or quantitated by phosphorimager analysis (Molecular Dynamics, Sunnyvale, CA).

RESULTS

In the presence of MgATP, *src* TK undergoes autophosphorylation (Barker et al., 1995). To map the site(s) of autophosphorylation, a technique was developed to rapidly digest *src* TK as well as other proteins (Lombardo et al., 1995). Recent advances in the ability to immobilize enzymes onto polystyrene, perfusive particles (PerSeptive Biosystems, Cambridge, MA) have enabled enzyme digests to proceed at much faster rates than previously possible, due principally to the ability to immobilize very high concentrations of a protease and to perform digestions on columns at elevated temperatures (Kassel et al., 1995). This advance has made it possible to generate complete enzymatic digestions of *src* TK within 2 min, allowing for the examination of phosphorylation as a function of time. Figure 1 shows a typical tryptic digest of an autophosphorylated sample of *src* TK using this technique. The peptide fragments are separated by HPLC and detected by ESI-MS. The elution times for three phosphotyrosine-containing peptides are shown in Figure 1. The fastest eluting phosphorylated fragment displayed a molecular mass of 1304 Da, which corresponded to residues 413−422, containing phosphorylation site Y419 (LIEDNE-pY-TAR). The second phosphorylated fragment yielded a molecular mass of 2656 Da, which corresponded to residues 225−346. MS/MS confirmed that Y338 was the only site of phosphorylation in this fragment (LVQLYAVVSEEPI-pY-IVTEYM-SK). The slowest eluting phosphorylated fragment yielded a molecular mass of 4079 Da, which corresponded to residues 504−536. MS/MS confirmed that Y530 was the only site of phosphorylation in this fragment (KEPEERPTFEY-LQAFLEDYFTSTEPQ-pY-QPGENL).

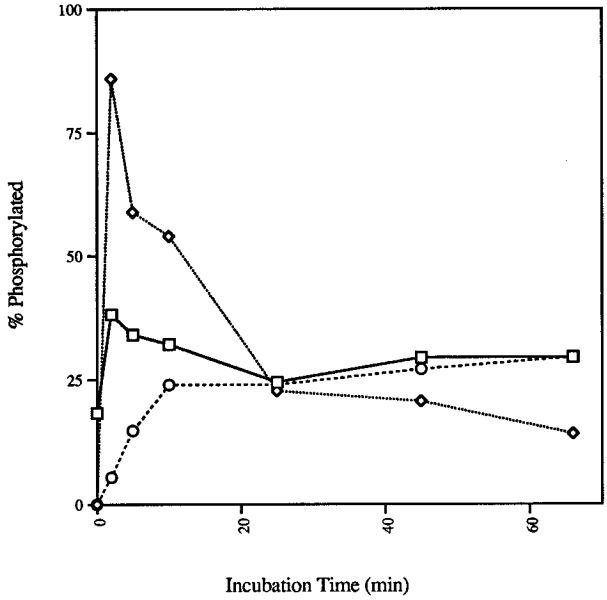

FIGURE 2: Autophosphorylation of individual tyrosine sites upon incubation of 10 μM *src* TK with 100 μM ATP and 20 mM $MgCl_2$ at 25 °C was examined as a function of time by ESI-MS. The percentage of tyrosine 419 (◇), tyrosine 338 (□), or tyrosine 530 (○) phosphorylated is shown.

The phosphorylation sites on untreated *src* TK without incubation with MgATP were also examined. A significant amount of phosphate was found incorporated in the tryptic digest fragment which corresponded to phosphorylation site Y338. A typical sample contained approximately 16% of Y338 phosphorylated. No other phosphotyrosine sites were found on untreated *src* TK.

Upon autophosphorylation of *src* TK with 100 μM ATP and 20 mM $MgCl_2$ at 25 °C, three phosphotyrosine-containing protein fragments were also detected. The peak areas from the phosphorylated and unphosphorylated forms of these three fragments were integrated to determine the relative percent phosphorylation. The percent phosphate content from all three tyrosine phosphorylation sites was summed and compared with the time course for autophosphorylation of *src* TK incubated with 100 μM [γ-^{32}P]ATP at 25 °C as monitored by measuring the amount of ^{32}P incorporated into *src* TK. Both methods showed that maximal autophosphorylation occurs within two min and is equivalent to approximately 1 mol of phosphate incorporated per mole of *src* TK. In addition, the amount of phosphate incorporated is relatively stable for the next 60 min.

Figure 2 shows the time course for the autophosphorylation of the three individual tyrosine sites found in *src* TK after incubation with 100 μM ATP at 25 °C. Maximal autophosphorylation of Y419 occurs within 2 min, followed by a

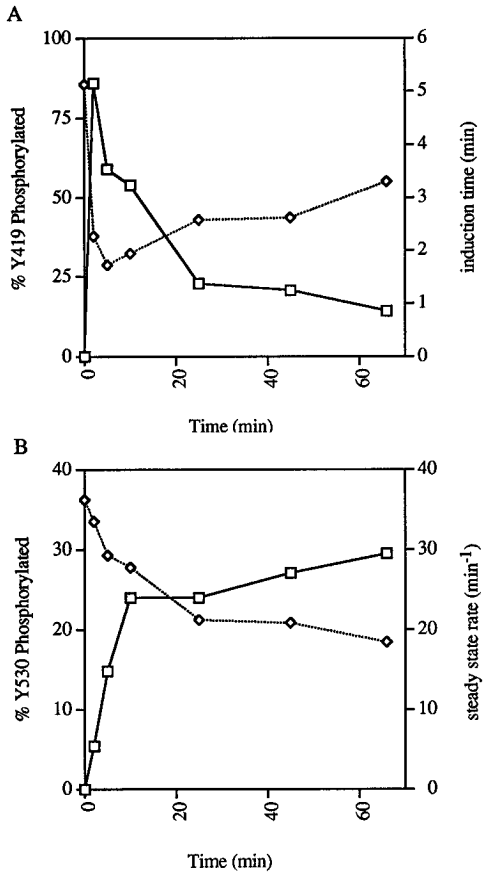

FIGURE 3: (A) Induction time determined from the tyrosine kinase continuous assay is plotted as a function of preincubation time (◇). Phosphorylation of tyrosine 419 from Figure 2 is overlaid (□). (B) The steady-state rate from the tyrosine kinase assay is plotted as a function of preincubation time (◇). The phosphorylation of tyrosine 530 from Figure 2 is overlaid (□).

decrease in its phosphorylation. Less than 20% of Y419 remained phosphorylated after 60 min in this experiment. Y338 and Y530 also become autophosphorylated. Maximal autophosphorylation of Y338 also occurs within 2 min, and slightly decreases during the following hour. An increase in phosphorylation of Y530 occurs throughout the entire time course. Although the total phosphorylation of the protein did not significantly change under these conditions, the phosphorylation of the individual sites changed dramatically.

The time course for autophosphorylation of *src* TK was compared with tyrosine kinase activity. A continuous spectrophotometric assay as described in Barker et al. (1995) was used to monitor *src* TK activity. Initially, a lag is seen in the reaction, which corresponds to the autoactivation of *src* TK. However, if *src* TK is fully activated prior to starting the reaction, no lag time is observed. The steady-state rate following the lag is proportional to the rate of phosphorylation of the peptide substrate. The intersection of the asymptotes of these two parts of the progress curve yields the induction time for autoactivation. Induction times were determined as a function of preincubation time (Figure 3A). For a comparison, the percentage of Y419 phosphorylated as a function of preincubation time (from Figure 2) was overlaid on the same graph as the induction time data. The data show that as Y419 is phosphorylated, the induction time decreases, and upon dephosphorylation of Y419, the induction time increases. These data provide direct evidence that the phosphorylation of Y419 leads to activation of *src* TK.

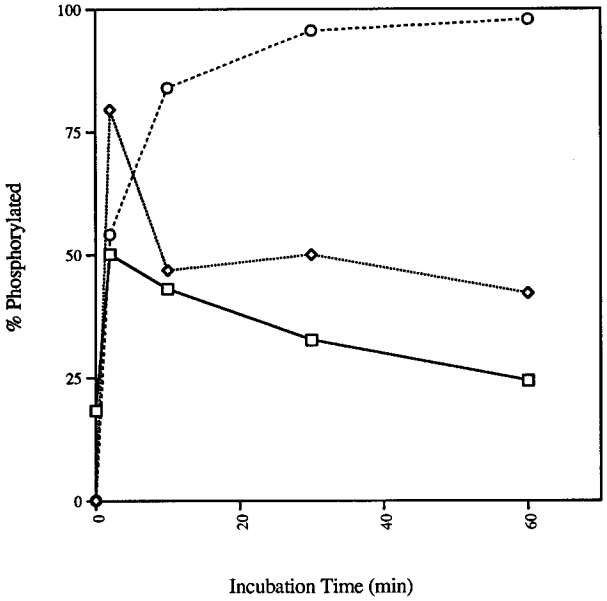

FIGURE 4: Autophosphorylation of individual tyrosine sites upon incubation of 10 μM *src* TK with 1 mM ATP and 20 mM $MgCl_2$ at 25 °C was examined as a function of time by ESI-MS. The pY530 enzyme used in subsequent experiments was generated by incubating for 60 min under these conditions. The percentage of tyrosine 419 (◇), tyrosine 338 (□), or tyrosine 530 (○) phosphorylated is shown.

The steady-state rate of peptide substrate phosphorylation was also determined as a function of preincubation time (Figure 3B). The percentage of Y530 phosphorylated as a function of preincubation time (from Figure 2) was overlaid in the same plot. Figure 3B shows that as Y530 is phosphorylated, the enzyme loses activity. These data support previous observations that the phosphorylation of Y530 leads to decreased *src* TK activity, but is in contrast to the proposal that it leads to complete inactivation (Cooper et al., 1986; Cooper & King, 1986; Cartwright et al., 1987; Kmiecik & Shalloway, 1987; Reynolds et al., 1987; Okada & Nakagawa, 1989).

Autophosphorylation conditions were also identified which resulted in complete phosphorylation of Y530 and partial phosphorylation of Y419 and Y338; this enzyme form is referred to as pY530 *src* TK. The time course for autophosphorylation of *src* TK upon incubation with 1 mM ATP and 20 mM $MgCl_2$ at 25 °C is shown in Figure 4. Untreated enzyme purified from baculovirus-infected insect cells contains only one phosphotyrosine site, Y338, which is typically 20−30% phosphorylated[2] (Barker et al., 1995). Maximal autophosphorylation of Y419 and Y338 occurs within 2 min, followed by dephosphorylation. However, there is a gradual decrease in the phosphorylation levels of Y419 and Y338, probably due to the ATP hydrolytic activity of *src* TK which could prevent the autophosphorylation/dephosphorylation reaction from reaching equilibrium (Barker et al., 1995; Boerner et al., 1995b). In contrast, the phosphorylation of Y530 approaches 100%. This is likely due to protection from dephosphorylation upon binding to the *src* SH2 domain rather than a dramatic difference in free energy, although this remains to be proven.

[2] *src* TK expressed in baculovirus-infected insect cells is also phosphorylated to a small extent on Y530. However, this phosphorylated form of the enzyme is separated out by ion exchange chromatography, leaving *src* TK which is only phosphorylated on Y338.

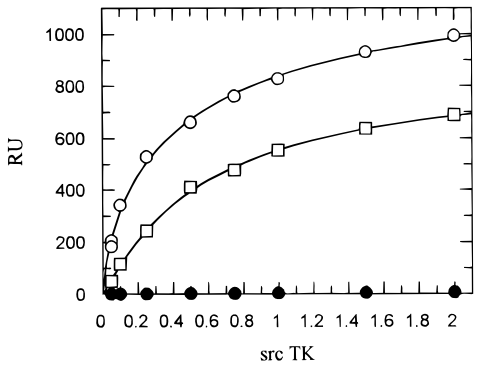

FIGURE 5: Surface plasmon resonance analysis of untreated (□), pY419 (○), and pY530 (●) *src* TK. The percent maximal response is plotted as a function of *src* TK concentration (μM).

Surface plasmon resonance analysis was used to determine the K_d for binding of a high-affinity SH2 ligand, TSTEPQ-pY-EEIENL (Gilmer et al., 1994), to the *src* SH2 domain in untreated *src* TK, pY530 *src* TK, as well as pY419 *src* TK. [The pY419 enzyme form was generated by incubating 10 μM *src* TK with 1 mM ATP and 20 mM $MgCl_2$ on ice for 60 min (Barker et al., 1995), and a typical sample contains 15%, 90%, and 2% of tyrosines 338, 419, and 530 phosphorylated, respectively.] Figure 5 shows that the K_d's for TSTEPQ-pY-EEIENL binding to untreated or pY419 enzyme were approximately 1.0 and 0.5 μM, respectively.[3] However, pY530 enzyme was unable to bind to TSTEPQ-pY-EEIENL under these same conditions. Analytical size exclusion chromatography demonstrated that untreated *src* TK, pY419 enzyme, and pY530 enzyme had similar retention times and corresponded to a monomeric species (data not shown), in agreement with a recent report showing that the purified, repressed form (phosphorylated on Y530) of *src* TK behaves as a monomer on a size exclusion column (Superti-Furga, 1995). These data support the model for an intramolecular association between phosphorylated Y530 and the SH2 domain (Matsuda et al., 1990). In addition, complete phosphorylation of Y530 led to essentially all of the enzyme forming the pY530−SH2 intramolecular complex as there was no detectable binding of pY530 *src* TK to the high-affinity SH2 ligand as measured by surface plasmon resonance.

The kinetic parameters of the pY530 *src* TK reaction were determined by the spectrophotometric assay (Table 1). The pY530 enzyme becomes autophosphorylated at Y419 in these studies, so the kinetic parameters are actually determined using *src* TK which contains essentially all of Y419 and Y530 phosphorylated.[4] The K_m for ATP was similar with the pY419 and pY530 enzymes, as was the K_m for peptide substrate. However, even though the pY530 enzyme contains essentially all of Y530 phosphorylated, the apparent k_{cat} was only 4−6 fold lower than the apparent k_{cat} for the pY419 enzyme. These results indicate that as long as Y419 is partially phosphorylated, *src* TK can autophosphorylate and phosphorylate peptide substrates, even though the enzyme is present as the pY530−SH2 intramolecular complex.

Table 1: Kinetic Parameters for pY419 and pY530 *Src* TK

enzyme form	varied substrate	K_m (μM)	app k_{cat} (min^{-1})
pY419[a]	ATP	148 ± 24[b]	26 ± 2
pY530[a]	ATP	97 ± 23[b]	6 ± 1
pY419[c]	ATP	134 ± 3[b]	744 ± 8
pY530[c]	ATP	76 ± 9[b]	118 ± 5
pY419[d]	$(FGE)_3Y(GEF)_2GD$	132 ± 22[e]	560 ± 50
pY530[d]	$(FGE)_3Y(GEF)_2GD$	85 ± 14[e]	95 ± 8

[a] Assayed with 250 μM RRLIEDAEYAARG and 0.2 μM *src* TK. [b] The K_m for ATP was previously determined to be 80−160 μM (Barker et al., 1995; Boerner et al., 1995a). [c] Assayed with 60 μM $(FGE)_3Y(GEF)_2GD$ and 3.9 nM *src* TK. [d] Assayed with 100 μM ATP and 3.9 nM *src* TK. [e] The K_m for $(FGE)_3Y(GEF)_2GD$ was previously determined to be 70−80 μM (Boerner et al., 1995a; Edison et al., 1995).

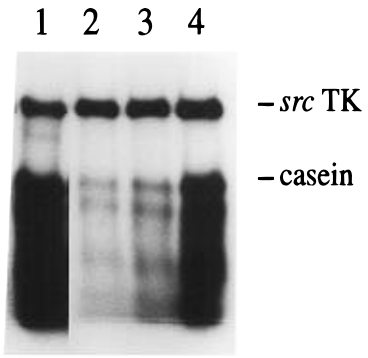

FIGURE 6: Phosphorylation of casein by *src* TK. Representative autoradiograph showing phosphorylation of casein by: lane 1, pY419 *src* TK; lane 2, pY530 *src* TK; lane 3, pY530 *src* TK in the presence of 50 μM TSTEPQ-pY-EEIENL; lane 4, pY530 *src* TK in the presence of 1 mM TSTEPQ-pY-EEIENL. *src* TK runs as a single band while casein contains multiple bands.

pY530 *src* TK can also phosphorylate casein, however, only 5−20% as effectively as the pY419 enzyme, consistent with the results obtained using a peptide substrate (Figure 6). Addition of TSTEPQ-pY-EEIENL at 1 mM, but not 50 μM, significantly increased the degree of casein phosphorylated by pY530 *src* TK to a level approximately the same as that observed with pY419 enzyme.

To determine the relative affinity of phosphorylated Y530 for the SH2 domain, activation of pY530 *src* tyrosine kinase activity by TSTEPQ-pY-EEIENL was examined as a function of the concentration of TSTEPQ-pY-EEIENL using the spectrophotometric tyrosine kinase assay with the peptide substrate RRLIEDAEYAARG (Figure 7). The data indicated saturation kinetics and a $K_{activation}$ for TSTEPQ-pY-EEIENL of approximately 200 μM. This value is approximately 200-fold greater than the K_d for binding of this peptide to the SH2 domain in untreated *src* TK. If we assume that the phosphopeptide only binds to the open form of the enzyme, then the 200-fold increase actually reflects an internal $K_{eq} \cong 200$ (unitless). Therefore, the pY530−SH2 interaction will decrease the ability of the phosphotyrosine

[3] It is not known why a smaller maximum response was achieved with unactivated *src* TK than with pY419 *src* TK. Differential maximal responses might be explained if the two forms of the enzyme could exist in different conformational states, which is likely, or if the pY419 enzyme was complexed with MgATP. However, this difference in maximal response has no influence on the actual K_d determination.

[4] Enzyme preparations containing 100% Y530 phosphorylated and variable levels of Y419 initially phosphorylated (≥40%), yield approximately 20% the activity of enzyme containing no Y530 phosphorylation. Upon addition of MgATP, the pY530 enzyme undergoes autophosphorylation on Y419. The observation of ^{32}P incorporation upon incubation of the pY530 enzyme with [γ-^{32}P]ATP supports this conclusion. Therefore, as long as some of the pY530 enzyme initially contains Y419 phosphorylated, the final phosphorylation state of Y419 will be the same in the assays and yield identical activity.

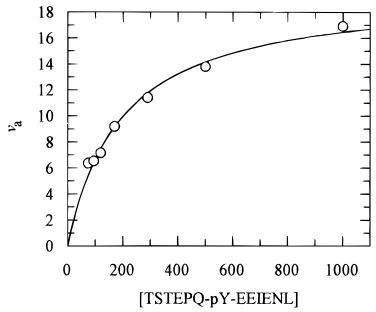

FIGURE 7: Activation of pY530 *src* tyrosine kinase activity by TSTEPQ-pY-EEIENL. The activated steady-state rate minus the unactivated rate (min^{-1}) is plotted as a function of peptide concentration (μM). The data were fit to eq 2 to determine a $K_{activation}$.

peptides and proteins to bind to the SH2 domain by this factor.

DISCUSSION

In this work, the time course for autophosphorylation of *src* TK on three tyrosine sites has been mapped using a rapid digestion technique involving perfusive-immobilized enzyme cartridges in combination with ESI-MS. This technique has allowed us to monitor modulation of phosphorylation states in *src* TK to help identify the effect of phosphorylation on activity.

In the spectrophotometric tyrosine kinase assay, the level of phosphorylation of Y419 was directly correlated with the time required for activation of *src* TK (induction time). The induction time increased upon dephosphorylation of Y419. Therefore, phosphorylation of Y419 is important for activating the kinase activity toward both itself and exogenous substrates. These results agree with mutagenesis experiments which showed that conversion of Y419 to phenylalanine decreased enzymatic activity as monitored by the spectrophotometric tyrosine kinase assay (Loganzo, Boerner, and Knight, unpublished results).

It has recently been shown that *src* TK isolated from a baculovirus expression system contains an additional tyrosine phosphorylation site, Y338 (Barker et al., 1995). Additionally, *src* TK can autophosphorylate Y338 *in vitro*. Although we have not identified whether or not phosphorylation of Y338 affects *src* TK activity, it is possible that phosphorylation of Y338 provides a docking site for other SH2 domain-containing protein(s). In turn, binding of a protein substrate to phosphorylated Y338 may facilitate catalysis by positioning tyrosine residues in close proximity to the *src* TK active site. This proposal is currently under study.

Src TK contains a third tyrosine site, Y530, which is thought to be phosphorylated predominantly by CSK TK (Okada & Nakagawa, 1989; Nada et al., 1991), but can also be autophosphorylated (Cooper & King, 1986; Cooper & MacAuley, 1988). Here, conditions were identified which promoted essentially complete autophosphorylation of Y530. Phosphorylation of Y530 was directly correlated to a decrease in tyrosine kinase activity. However, even when the protein is approximately 100% phosphorylated on Y530 and phosphorylated on Y419, about 20% of the kinase activity is retained regardless of whether a peptide or protein substrate was used. Interestingly, the K_m's for MgATP or peptide substrate are not affected by phosphorylation of Y530.

Surface plasmon resonance studies demonstrate that phosphorylation of Y530 is directly responsible for inhibiting binding of the *src* SH2 domain to a high-affinity peptide ligand. In addition, the phosphorylated Y530 enzyme is present as a monomer, supporting the model for an intramolecular association between phosphorylated Y530 and the SH2 domain (Matsuda et al., 1990). These results indicate that formation of the pY530−SH2 intramolecular interaction is not sufficient to abolish tyrosine kinase activity with the N-85 *src* TK protein construct. In fact, when a full-length *src* TK protein construct which lacks only its myristylation site was used, phosphorylation of Y530 still led to an intramolecular complex which retained approximately 20% tyrosine kinase activity. However, it is possible that in the absence of any phosphorylation on Y419, phosphorylation of Y530 and formation of the pY530−SH2 intramolecular complex could inactivate *src* tyrosine kinase activity since this could prevent an initial intramolecular autophosphorylation event that initiates intermolecular autophosphorylation. Furthermore, the pY530−SH2 intramolecular interaction inhibits the ability of an SH2 ligand to bind to the SH2 domain by a factor of 200. Therefore, phosphorylation of Y530 by either CSK TK or *src* TK modulates signal transduction by down-regulating *src* TK activity and, importantly, by inhibiting the association of other signal-transducing proteins with the *src* SH2 and SH3 domains.

In terms of drug development, inhibitors aimed at blocking binding to the *src* SH2 domain should be effective in stopping aberrant cell signaling. The data reported in this work indicate that inhibitors will actually be 200-fold more potent in transformed cells versus activated *src* TK than in "normal" cells which contain *src* TK in its repressed state (with Y530 phosphorylated and present as the pY530−SH2 intramolecular complex). This 200-fold window suggests that the ligands will not lead to activation of *src* tyrosine kinase activity in normal cells and therefore will lead to minimal nonselective cytotoxicity. This has been a concern in the development of this class of inhibitors, i.e., would SH2 ligands lead to activation of repressed *src* TK in normal cells? Therefore, drug targets aimed at binding to the SH2 domain of *src* TK are likely to be effective and selective in treating breast and colon carcinomas.

REFERENCES

Barker, S. C., Kassel, D. B., Weigl, D., Huang, X., Luther, M., & Knight, W. B. (1995) *Biochemistry 34*, 14843−14851.

Boerner, R. J., Barker, S. C., & Knight, W. B. (1995a) *Biochemistry 34*, 16419−16423.

Boerner, R. J., Kassel, D. B., Edison, A. M., & Knight, W. B. (1995b) *Biochemistry 34*, 14852−14860.

Bolen, J. B. (1993) *Oncogene 8*, 2025−2031.

Cantley, L. C., Auger, K. R., Carpenter, C., Duckworth, B., Graziani, A., Kapeller, R., & Soltoff, S. (1991) *Cell 64*, 281−302.

Cartwright, C. H., Eckhart, W., Simon, S., & Kaplan, P. L. (1987) *Cell 49*, 83−91.

Cooper, J. A., & King, C. S. (1986) *Mol. Cell. Biol. 6*, 4467−4477.

Cooper, J. A., & MacAuley, A. (1988) *Proc. Natl. Acad. Sci. U.S.A. 85*, 4232−4236.

Cooper, J. A., & Howell, B. (1993) *Cell 73*, 1051−1054.

Cooper, J. A., Gould, K. L., Cartwright, C. A., & Hunter, T. (1986) *Science 231*, 1431−1434.

Edison, A. M., Barker, S. C., Kassel, D. B., Luther, M. A., & Knight, W. B. (1995) *J. Biol. Chem. 270*, 27112−27115.

Ellis, B., DeLacy, P., Weigl, D., Kassel, D., Patel, I., Wisely, G. B., Lewis, K., Overton, L., Kadwell, S., Kost, T., Hoffman, C., Barrett, G., Robbins, J., Knight, W. B., Edison, A., Huang, X., Berman, J., Rodriquez, M., & Luther, M. (1994) *J. Cell. Biochem. Suppl. 18B*, 276.

Fagerstam, L. G., Frostell-Karlsson, A., Karlsson, R., Persson, B., & Ronnberg, I. (1992) *J. Chromatogr. 597*, 397−410.

Gilmer, T., Rodriguez, M., Jordan, S., Crosby, R., Alligood, K., Green, M., Kimery, M., Wagner, C., Kinder, D., Charifson, P., Hassell, A. M., Willard, D., Luther, M., Rusnak, D., Sternbach, D., Mehrotra, M., Peel, M., Shampine, L., Davis, R., Robbins, J., Patel, I. R., Kassel, D., Burkhart, W., Moyer, M., Bradshaw, T., & Berman, J. (1994) *J. Biol. Chem. 269*, 31711−31719.

Kassel, D. B., Consler, T. G., Shalaby, M., Sekhri, P., Gordon, N., & Nadler, T. (1995) in *Techniques in Protein Chemistry VI* (Crabb, J. W., Eds.) Academic Press, New York.

Kmiecik, T. E., & Shalloway, D. (1987) *Cell 49*, 65−73.

Laemmli, U. K. (1970) *Nature 227*, 680−685.

Leatherbarrow, R. J. (1992) *GraFit* Version 3.0, Erithacus Software Ltd., Staines, U.K.

Lombardo, C. R., Consler, T. G., & Kassel, D. B. (1995) *Biochemistry 34*, 16456−16466.

Malmquist, M. (1993) *Curr. Opin. Immunol. 5*, 282−286.

Matsuda, M., Mayer, B. J., Fukui, Y., & Hanafusa, H. (1990) *Science 248*, 1537−1539.

Nada, S., Okada, M., MacAuley, A., Cooper, J. A., & Nakagawa, H. (1991) *Nature 351*, 69−72.

Okada, M., & Nakagawa, H. (1989) *J. Biol. Chem. 264*, 20886−20893.

Reynolds, A. B., Vila, J., Lansing, T. J., Potts, W. M., Weber, M. J., & Parsons, J. T. (1987) *EMBO J. 6*, 2359−2364.

Sudol, M. (1993) in *The Molecular Basis of Human Cancer* (Neel, B., & Kumar, R., Eds.) Futura Publishing Co. Inc., Mount Kisco, NY.

Superti-Furga, G. (1995) *FEBS Lett. 369*, 62−66.

BI960248U